Scaling laws for single-file diffusion of adhesive particles

Sören Schweers [1,*] Alexander P. Antonov [1,†] Artem Ryabov [2,‡] and Philipp Maass [1,§]

[1]*Universität Osnabrück, Fachbereich Physik, Barbarastraße 7, D-49076 Osnabrück, Germany*
[2]*Charles University, Faculty of Mathematics and Physics, Department of Macromolecular Physics,*
V Holešovičkách 2, CZ-18000 Praha 8, Czech Republic

Single-file diffusion refers to the Brownian motion in narrow channels where particles cannot pass each other. In such processes, the diffusion of a tagged particle is typically normal at short times and becomes subdiffusive at long times. For hard-sphere interparticle interaction, the time-dependent mean squared displacement of a tracer is well understood. Here we develop a scaling theory for adhesive particles. It provides a full description of the time-dependent diffusive behavior with a scaling function that depends on an effective strength of adhesive interaction. Particle clustering induced by the adhesive interaction slows down the diffusion at short times, while it enhances subdiffusion at long times. The enhancement effect can be quantified in measurements irrespective of how tagged particles are injected into the system. Combined effects of pore structure and particle adhesiveness should speed up translocation of molecules through narrow pores.

Diffusive motion in narrow pores is an important process in many biological, chemical, and engineering systems. When particles in these confined structures cannot overtake each other, the process is referred to as single-file diffusion [1–4]. Prominent examples are the tracer diffusion in zeolites [5–7], in colloidal systems [8–15], nanotubes [16–20], in membrane channels and pores [21–26], and in a macroscopic system of electrically interacting metallic beads confined to a ring [27]. In the long-time limit the mean squared displacement $\langle \Delta x^2(t) \rangle$ of a tagged particle in single-file diffusion does not grow linearly but with the square root of time t [28–38],

$$\langle \Delta x^2(t) \rangle \sim 2D_{1/2}\sqrt{t}, \quad \text{for } t \to \infty. \quad (1)$$

The coefficient $D_{1/2}$ quantifies the speed of the spreading similarly as the diffusion coefficient in normal diffusion.

Generally, the mean squared displacement shows a crossover from a normal diffusive behavior $\langle \Delta x^2(t) \rangle \sim 2Dt$ at short times to the subdiffusive law (1) at long times. In simple systems, one could expect the crossover time $t_\times$ between the normal and subdiffusive regime to be determined by the condition that the root of the mean squared displacement equals the mean distance $1/\rho$ between particles, where ρ is the particle number density. This gives $2Dt_\times \sim 1/\rho^2$, and by matching $2Dt_\times$ with $2D_{1/2}t_\times^{1/2}$, one obtains $D_{1/2} \sim \sqrt{D}/\rho$. In lattice systems at low densities, or continuous space systems of point particles, this relation between D and $D_{1/2}$ is indeed often obtained [30,33,39,40].

Less is known about the behavior of the mean squared displacement in single-file systems of particles with attractive and repulsive interactions. A prominent model to capture major characteristics of real interactions with a repulsive core and adhesive part is the model of sticky hard spheres [41,42], where the pair interaction $V(r)$ between particles is given by

$$\exp[-V(r)/k_\text{B}T] = \Theta(r-\sigma) + \gamma\sigma\delta_+(r-\sigma). \quad (2)$$

Here, σ is the particle diameter, $k_\text{B}T$ is the thermal energy, $\Theta(.)$ is the Heaviside step function [$\Theta(x) = 1$ for $x > 0$ and zero otherwise], and $\delta_+(r)$ is the right-sided δ-function, i.e., for any test function $h(r)$ and $\epsilon > 0$, it holds $\int_0^\epsilon dr\, h(r)\delta_+(r) = h(0)$. The Heaviside function $\Theta(r-\sigma)$ in Eq. (2) implies that $V(r)$ is infinite for $r < \sigma$, i.e., it takes into account the hardcore repulsion. The function $\gamma\sigma\delta_+(r-\sigma)$ describes an additional attractive contact interaction, where $\gamma\sigma$ quantifies the adhesive strength. We refer to the dimensionless parameter γ as the stickiness.

In this Letter we show that the mean squared displacement of sticky hard spheres in single-file systems can be described by scaling laws, where the scaling function depends on an effective stickiness parameter between the spheres, which combines γ with the particle number density ρ. Exact results are given for the limiting behavior of the scaling function at short and long scaled times. The coefficient $D_{1/2}$ in Eq. (1) is proportional to the square root of the isothermal compressibility of the system, as can be inferred from a general result for the long-time asymptotics [32], including the case of underdamped Brownian motion [43]. The dependence on the compressibility implies that subdiffusion becomes faster for attractive and slower for repulsive interactions. This is in contrast to what is typically found in normal diffusion and different from what has been seen for single-file diffusion in some one-dimensional lattice models with attractive interactions [44,45].

---

*sschweers@uos.de
†alantonov@uos.de
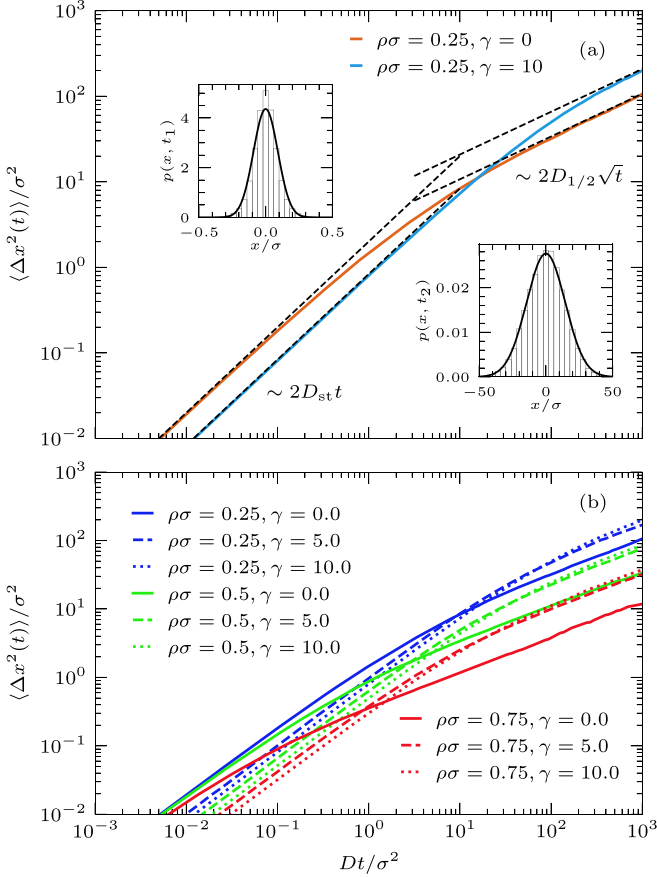‡rjabov.a@gmail.com
§maass@uos.de

FIG. 1. (a) Mean squared displacement of a tagged particle for scaled density (coverage) $\rho\sigma = 0.25$ in the absence of adhesive interactions ($\gamma = 0$) and for stickiness $\gamma = 10$. The insets show the diffusion propagator at fixed times in the short-time regime ($Dt_1/\sigma^2 = 10^{-2}$) and the long-time regime ($Dt_2/\sigma^2 = 10^3$) for $\gamma = 10$. (b) Mean squared displacement for various $\rho\sigma$ and γ.

The overdamped Brownian motion of the particles with positions x_i, $i = 1, \ldots, N$ is described by the Langevin equations

$$\frac{dx_i}{dt} = \sqrt{2D}\,\xi_i(t), \tag{3}$$

where D is the bare diffusion coefficient and $\xi_i(t)$ are Gaussian white noise processes with zero mean and correlation functions $\langle\xi_i(t)\xi_j(t')\rangle = \delta_{ij}\delta(t - t')$. The treatment of the hardcore and adhesive interactions needs special care due to their singular nature. We have applied our recently developed Brownian cluster dynamics algorithm to tackle this problem [46]. For determining equilibrium properties, we have also performed Monte Carlo simulations based on the method developed in Refs. [47,48].

Figure 1(a) shows simulation results for $\langle\Delta x^2(t)\rangle$ at one number density $\rho = 1/4\sigma$ for strong adhesive interaction $\gamma = 10$ and for $\gamma = 0$ [49]. The initial distribution of the tagged particle is the equilibrium one. In an equilibrium configuration, the tagged particle can be part of different clusters of particles in contact. A sequence of particles with positions $x_i = x_1 + (i - 1)\sigma$, $i = 1, \ldots, n$ and no particles at positions

$x_1 - \sigma$ and $x_n + \sigma$ forms a cluster of size n (n-cluster); single particles are 1-clusters.

At short times, the motion of clusters is not affected by the presence of neighboring clusters and $\langle\Delta x^2(t)\rangle$ grows linearly in time, corresponding to normal diffusion. At long times, the mean square displacement shows the subdiffusion characteristic for single-file Brownian motion, $\langle\Delta x^2(t)\rangle \sim t^{1/2}$. In the insets of Fig. 1(a), we display the diffusion propagator $p(x, t)$ at two fixed times in the short- and long-time regime. For all times, this propagator is a Gaussian function, $p(x, t) \propto \exp[-x^2/2\langle\Delta x^2(t)\rangle]$. Note that $\langle\Delta x^2(t)\rangle$ at long times is enhanced by the adhesive interaction. This speedup of subdiffusion may be unexpected at first sight because attractive particle interactions usually slow down Brownian motion.

Figure 1(b) shows simulation results for various $\rho\sigma$ and γ. The speed-up effect is always present, which can be seen by comparing the curves for different γ (same color) at fixed $\rho\sigma$ values (solid, dashed, or dotted lines). The change of functional behavior of $\langle\Delta x^2(t)\rangle$ with $\rho\sigma$ and γ seems to be complicated.

We now develop a scaling theory that fully describes the behavior of $\langle\Delta x^2(t)\rangle$ in this many-body system. We start by determining the behavior in the short-time limit $t \to 0$, which can be inferred from the distribution of cluster sizes in the equilibrium state. To derive the cluster size distribution, we can build on exact results for thermodynamic and structural properties of the sticky-core fluid in equilibrium [50–52]. For the pair correlation function, it was found that [52]

$$g(r) = \frac{1}{\rho}\sum_{n=1}^{\infty}\{q^n\delta_+(r - n\sigma) + f_n(r - n\sigma)\Theta(r - n\sigma)\}, \tag{4}$$

where $f_n(r)$ are smooth functions of r, and

$$q = \frac{\sqrt{1 + 4\tilde{\gamma}} - 1}{\sqrt{1 + 4\tilde{\gamma}} + 1} \tag{5}$$

with

$$\tilde{\gamma} = \frac{\gamma\rho\sigma}{1 - \rho\sigma}. \tag{6}$$

This dimensionless parameter is the stickiness multiplied by the ratio of particle diameter σ to the mean size $1/\rho - \sigma$ of free space between particles. It describes the effective stickiness.

As shown in the Supplemental Material (SM) [53], the δ functions in Eq. (4) with the amplitudes q^n/ρ follow if the cluster size distribution is the geometric distribution

$$w_n = (1 - q)q^{n-1}. \tag{7}$$

The mean cluster size then is given by

$$\bar{n}(\tilde{\gamma}) = \frac{1}{1 - q} = \frac{1}{2}(\sqrt{1 + 4\tilde{\gamma}} + 1). \tag{8}$$

Both Eqs. (7) and (8) agree with the simulated data, see the SM.

Initially, the tagged particle is part of an n-cluster with probability $\propto nw_n$, and the center of mass of this n-cluster has a diffusion constant D/n. Accordingly, the short-time diffusion coefficient D_{st} of the tagged particle is obtained by

averaging D/n over the distribution $\propto n w_n$, yielding

$$D_{\mathrm{st}}(\tilde{\gamma}, \rho\sigma) = \frac{D}{\bar{n}(\tilde{\gamma})} = \frac{2D}{\sqrt{1 + \frac{4\gamma\rho\sigma}{1-\rho\sigma}} + 1} . \qquad (9)$$

When time increases, the Brownian motion of the tagged particle becomes mitigated due to the hindrance of free diffusion by neighboring particles, leading to subdiffusion as described by Eq. (1).

For determining the dependence of $D_{1/2}(\tilde{\gamma}, \rho\sigma)$ on $\tilde{\gamma}$ and $\rho\sigma$, let us first consider a situation, where fragmentations and mergers of the initial clusters during the course of time are neglected. This situation corresponds to a diffusion of a tagged particle in a random mixture of clusters with different fixed sizes given by the geometric distribution (7).

To derive the diffusion coefficient of a tagged particle in this cluster mixture, we use scaling arguments. If all clusters are represented by ones having the same mean size $\bar{n}$, the crossover from the normal diffusive behavior at short times to the subdiffusive one at long times will occur when the root mean square displacement becomes proportional to the average spacing between the clusters. Accordingly, the root of the mean squared displacement at the crossover time $t_\times$ should be proportional to $\bar{n}(1/\rho - \sigma)$. This implies $2D_{\mathrm{st}} t_\times \sim [\bar{n}(\tilde{\gamma})(1/\rho - \sigma)]^2$, yielding

$$t_\times(\tilde{\gamma}, \rho\sigma) \sim \frac{[\bar{n}(\tilde{\gamma})(1/\rho - \sigma)]^2}{2D_{\mathrm{st}}(\tilde{\gamma}, \rho\sigma)} = \frac{\bar{n}(\tilde{\gamma})^3(1-\rho\sigma)^2}{2D\rho^2} . \quad (10)$$

Knowing $t_\times$, we expect the mean squared displacement to obey the following scaling behavior,

$$\langle \Delta x^2(t) \rangle = \bar{n}(\tilde{\gamma})^2 \frac{(1-\rho\sigma)^2}{\rho^2} F\left(\frac{t}{t_\times(\tilde{\gamma}, \rho\sigma)} \right). \qquad (11)$$

Here, $F(u)$ is a scaling function with $F(u) \sim u$ for $u \to 0$ and $F(u) \sim F^\infty u^{1/2}$ for $u \to \infty$, where F^∞ is a constant. In the limit of hardcore interacting point particles ($\sigma = 0$, $\gamma = 0$), we obtain $\tilde{\gamma} = 0$ and $\bar{n}(\tilde{\gamma} = 0) = 1$, and it is known that $D_{1/2} = \sqrt{D/\pi}/\rho$ for equilibrated configurations [28,29,33,39,40]. Accordingly, it must hold $F^\infty = \sqrt{2/\pi}$. Simulations for the system with fixed cluster sizes confirm the scaling behavior predicted by Eq. (11), see the SM.

Turning back to the system of adhesive particles, the short-time diffusion coefficient in Eq. (9) must describe the behavior in the limit $t \to 0$, but we cannot expect $D_{\mathrm{st}}(\tilde{\gamma}, \rho\sigma)$ to be unaffected by the possible fragmentation and mergers of clusters in the whole short-time regime $t \lesssim t_\times$.

However, our analysis above suggests that mean squared displacements can be scaled along a curve in the $\rho\gamma$ plane, where the effective stickiness $\tilde{\gamma}$ is constant. The scaling (11) should hold for $\langle \Delta x^2(t) \rangle$ along such curves, with a $\tilde{\gamma}$-dependent scaling function $F_{\tilde{\gamma}}(t/t_\times(\tilde{\gamma}, \rho\sigma))$. The functional behavior of $F_{\tilde{\gamma}}(u)$ for $u \to 0$ and $u \to \infty$ must be unchanged, but we now have to consider a $\tilde{\gamma}$-dependent amplitude factor $F_{\tilde{\gamma}}^\infty$.

Figures 2(a) and 2(b) show correspondingly scaled simulation data of the mean square displacements for various ρ and γ at fixed $\tilde{\gamma} = 0.2$ [Fig. 2(a)] and $\tilde{\gamma} = 2$ [Fig. 2(b)]. They are in excellent agreement with the scaling prediction. The inset in Fig. 2(b) shows that the scaling functions $F_{\tilde{\gamma}=2}(u)$ and $F_{\tilde{\gamma}=0.2}(u)$ are equal for small u, but differ for larger u. Within
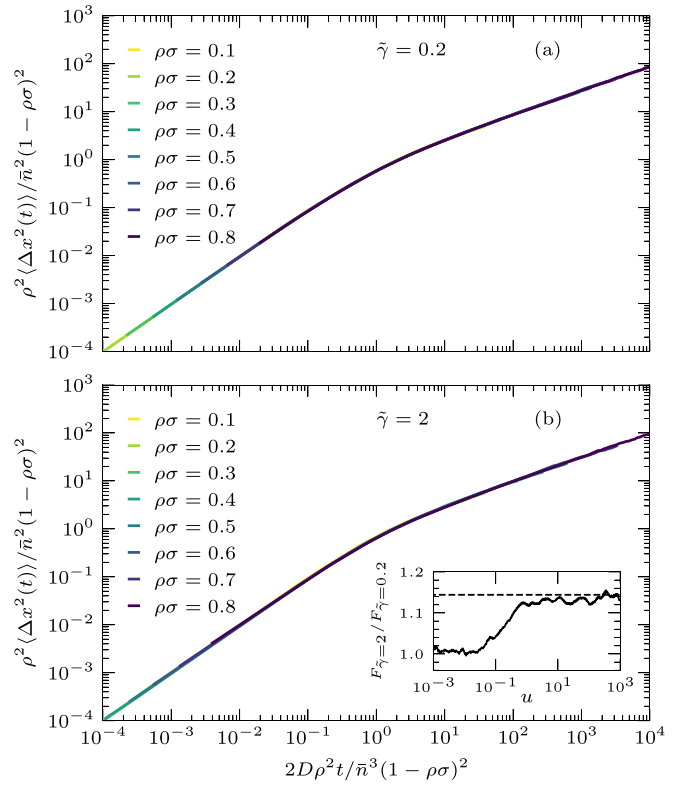

FIG. 2. Scaled mean squared displacement as a function of scaled time according to Eq. (11). For (a) fixed $\tilde{\gamma} = 0.2$ and (b) fixed $\tilde{\gamma} = 2$, the data for various densities ρ and adhesive strengths $\gamma = (1/\rho\sigma - 1)\tilde{\gamma}$ collapse onto common master curves [γ varies according to Eq. (6)]. The inset in (b) shows the ratio $F_{\tilde{\gamma}=2}(u)/F_{\tilde{\gamma}=0.2}(u)$ of the two scaling functions, which increases from one for $u \to 0$ to the constant value 1.144 predicted by Eq. (13) for $u \to \infty$. The constant is indicated by the dashed horizontal line.

the numerical uncertainties, the ratio $F_{\tilde{\gamma}=2}(u)/F_{\tilde{\gamma}=0.2}(u)$ increases monotonically from one for small u to a value of about 1.14 for large u.

Surprisingly, we can determine the limit $F_{\tilde{\gamma}}^\infty$ of the scaling function $F_{\tilde{\gamma}}(u)$ from equilibrium properties. This is due to the fact that the coefficient $D_{1/2}$ in Eq. (1) can be expressed by D, ρ and the isothermal compressibility χ [32,39]. For the adhesive particle system, χ is known and we obtain (for details, see the SM)

$$D_{1/2}(\tilde{\gamma}, \rho\sigma) = \sqrt{\frac{k_{\mathrm{B}}T\chi D}{\pi\rho}} = \frac{1-\rho\sigma}{\sqrt{\pi}\rho} \sqrt{[2\bar{n}(\tilde{\gamma}) - 1]D}. \quad (12)$$

For long times, $2D_{1/2}t^{1/2}$ must equal the asymptotic behavior of Eq. (11). Taking $t_\times(\tilde{\gamma}, \rho\sigma)$ from Eq. (10), this yields

$$F_{\tilde{\gamma}}^\infty = \sqrt{\frac{2}{\pi}\left[2 - \frac{1}{\bar{n}(\tilde{\gamma})}\right]}. \qquad (13)$$

This function is weakly increasing from the point-particle limit $F_{\tilde{\gamma}=0}^\infty = \sqrt{2/\pi}$ to $F_{\tilde{\gamma}=\infty}^\infty = \sqrt{2}F_{\tilde{\gamma}=0}^\infty$ for strong adhesive interaction or, more precisely, strong effective stickiness $\tilde{\gamma}$. In agreement with Eq. (13), the simulated data of $F_{\tilde{\gamma}=2}(u)/F_{\tilde{\gamma}=0.2}(u)$ for large u approach the limit $F_{\tilde{\gamma}=2}^\infty/F_{\tilde{\gamma}=0.2}^\infty \cong 1.144$, see the inset of Fig. 2(b).

In summary we have developed a scaling theory for the time-dependent mean squared displacement of a tagged particle in single-file diffusion of adhesive hard spheres. The scaling applies to curves in the plane of stickiness and particle densities, where the effective stickiness is constant. The effective stickiness is the product of stickiness and the ratio of particle diameter to mean size of free space between particles. Due to the adhesion, particles gather in clusters with sizes distributed according to a geometric distribution, where the mean cluster size increases with the effective stickiness. The clustering slows down the normal diffusive behavior at short times, i.e., the short-time diffusion coefficient decreases with increasing adhesive strength. By contrast, the subdiffusion at long-times is sped up with raising adhesive strength because collective density fluctuations are decisive for the tracer to propagate over long distances. These density fluctuations become stronger if the particles form clusters and the mean free space between clusters becomes larger. The crossover from the normal to the subdiffusive regime occurs at a time, which increases with the third power of the mean cluster size and is thus growing with the adhesiveness.

The effect of the density fluctuations on the coefficient $D_{1/2}$ characterizing the speed of the subdiffusive spreading can be fully taken into account by considering their long-wavelength behavior, which is given by the zero-wave number limit of the static structure factor $S(0)$ [32]. The latter is related to the isothermal compressibility χ, $S(0) = k_B T \rho \chi$. For hardcore interacting particles, the important role of the compressibility has been pointed out already in early studies of single-file diffusion [39].

An interesting aspect of the dependence of $D_{1/2}$ on $S(0)$ concerns the impact of initial conditions: what matters for $D_{1/2}$ is the initial arrangement of the particles in the system, while the initial placement of the tagged particle is irrelevant. In our simulations of sticky hard spheres, we show this independence of $D_{1/2}$ on the initial starting position of the tagged particle in the SM. For measurements this implies that particles injected as, e.g., radioactive or fluorescent-labeled tracers, need not to be equilibrated with the surrounding structure.

Furthermore, the sensitivity of $D_{1/2}$ to $S(0)$ can be important to understand different speeds of subdiffusion, as reflected, for example, in traversal times of particles through pores. One may also think of utilizing this effect: a patterning of a channel leading to a larger particle separation or a clustering of particles should facilitate the diffusive motion through the channel. Systematic investigations of such pattern-induced enhancement of single-file diffusion and the effects of stickiness should be possible, e.g., in microfluidic devices [54,55]. For adhesive particles, it is in particular interesting to also study the short-time regime, where the adhesiveness and particle clustering can be determined from the short-time diffusion coefficient.

[1] J. Kärger, Transport phenomena in nanoporous materials, ChemPhysChem **16**, 24 (2015).

[2] K. Nygård, Colloidal diffusion in confined geometries, Phys. Chem. Chem. Phys. **19**, 23632 (2017).

[3] A. Taloni, O. Flomenbom, R. Castañeda-Priego, and F. Marchesoni, Single file dynamics in soft materials, Soft Matter **13**, 1096 (2017).

[4] B. C. Bukowski, F. J. Keil, P. I. Ravikovitch, G. Sastre, R. Q. Snurr, and M.-O. Coppens, Connecting theory and simulation with experiment for the study of diffusion in nanoporous solids, Adsorption **27**, 683 (2021).

[5] K. Hahn, J. Kärger, and V. Kukla, Single-File Diffusion Observation, Phys. Rev. Lett. **76**, 2762 (1996).

[6] K. Hahn and J. Kärger, Deviations from the normal time regime of single-file diffusion, J. Phys. Chem. B **102**, 5766 (1998).

[7] C. Chmelik, J. Caro, D. Freude, J. Haase, R. Valiullin, and J. Kärger, Diffusive Spreading of Molecules in Nanoporous Materials, in *Diffusive Spreading in Nature, Technology and Society*, edited by A. Bunde, J. Caro, J. Kärger, and G. Vogl (Springer International Publishing, Cham, 2018), Chap. 10, pp. 171–202.

[8] Q.-H. Wei, C. Bechinger, and P. Leiderer, Single-file diffusion of colloids in one-dimensional channels, Science **287**, 625 (2000).

[9] B. Cui, H. Diamant, and B. Lin, Screened Hydrodynamic Interaction in a Narrow Channel, Phys. Rev. Lett. **89**, 188302 (2002).

[10] B. Lin, B. Cui, J.-H. Lee, and J. Yu, Hydrodynamic coupling in diffusion of quasi–one-dimensional brownian particles, Europhys. Lett. **57**, 724 (2002).

[11] C. Lutz, M. Kollmann, and C. Bechinger, Single-File Diffusion of Colloids in One-Dimensional Channels, Phys. Rev. Lett. **93**, 026001 (2004).

[12] C. Lutz, M. Kollmann, P. Leiderer, and C. Bechinger, Diffusion of colloids in one-dimensional light channels, J. Phys.: Condens. Matter **16**, S4075 (2004).

[13] B. Lin, M. Meron, B. Cui, S. A. Rice, and H. Diamant, From Random Walk to Single-File Diffusion, Phys. Rev. Lett. **94**, 216001 (2005).

[14] M. Köppl, P. Henseler, A. Erbe, P. Nielaba, and P. Leiderer, Layer Reduction in Driven 2D-Colloidal Systems through Microchannels, Phys. Rev. Lett. **97**, 208302 (2006).

[15] P. Henseler, A. Erbe, M. Köppl, P. Leiderer, and P. Nielaba, Density reduction and diffusion in driven two-dimensional colloidal systems through microchannels, Phys. Rev. E **81**, 041402 (2010).

[16] C.-Y. Cheng and C. R. Bowers, Observation of single-file diffusion in dipeptide nanotubes by continuous-flow hyperpolarized Xenon-129 NMR spectroscopy, ChemPhysChem **8**, 2077 (2007).

[17] A. Das, S. Jayanthi, H. S. M. V. Deepak, K. V. Ramanathan, A. Kumar, C. Dasgupta, and A. K. Sood, Single-file diffusion of confined water inside SWNTs: An NMR study, ACS Nano **4**, 1687 (2010).

[18] M. Dvoyashkin, H. Bhase, N. Mirnazari, S. Vasenkov, and C. R. Bowers, Single-file nanochannel persistence lengths from NMR, Anal. Chem. **86**, 2200 (2014).

[19] W. Cao, L. Huang, M. Ma, L. Lu, and X. Lu, Water in narrow carbon nanotubes: Roughness promoted diffusion transition, J. Phys. Chem. C **122**, 19124 (2018).

[20] S. Zeng, J. Chen, X. Wang, G. Zhou, L. Chen, and C. Dai, Selective transport through the ultrashort carbon nanotubes embedded in lipid bilayers, J. Phys. Chem. C **122**, 27681 (2018).

[21] W. R. Bauer and W. Nadler, Molecular transport through channels and pores: Effects of in-channel interactions and blocking, Proc. Natl. Acad. Sci. USA **103**, 11446 (2006).

[22] M. Kahms, P. Lehrich, J. Hüve, N. Sanetra, and R. Peters, Binding site distribution of nuclear transport receptors and transport complexes in single nuclear pore complexes, Traffic **10**, 1228 (2009).

[23] S. Y. Yang, J.-A. Yang, E.-S. Kim, G. Jeon, E. J. Oh, K. Y. Choi, S. K. Hahn, and J. K. Kim, Single-file diffusion of protein drugs through cylindrical nanochannels, ACS Nano **4**, 3817 (2010).

[24] B. Luan and R. Zhou, Single-file protein translocations through graphene–mos2 heterostructure nanopores, J. Phys. Chem. Lett. **9**, 3409 (2018).

[25] M. Zhao, W. Wu, and B. Su, ph-controlled drug release by diffusion through silica nanochannel membranes, ACS Appl. Mater. Interfaces **10**, 33986 (2018).

[26] J. Kärger, D. M. Ruthven, and R. Valiullin, Diffusion in nanopores: inspecting the grounds, Adsorption **27**, 267 (2021).

[27] C. Coste, J.-B. Delfau, C. Even, and M. Saint Jean, Single-file diffusion of macroscopic charged particles, Phys. Rev. E **81**, 051201 (2010).

[28] T. E. Harris, Diffusion with "collisions" between particles, J. Appl. Probab. **2**, 323 (1965).

[29] D. G. Levitt, Dynamics of a single-file pore: Non-Fickian behavior, Phys. Rev. A **8**, 3050 (1973).

[30] R. Arratia, The motion of a tagged particle in the simple symmetric exclusion system on $\mathbb{Z}^1$, Ann. Probab. **11**, 362 (1983).

[31] K. Hahn and J. Kärger, Molecular dynamics simulation of single-file systems, J. Phys. Chem. **100**, 316 (1996).

[32] M. Kollmann, Single-file Diffusion of Atomic and Colloidal Systems: Asymptotic Laws, Phys. Rev. Lett. **90**, 180602 (2003).

[33] L. Lizana and T. Ambjörnsson, Single-File Diffusion in a Box, Phys. Rev. Lett. **100**, 200601 (2008).

[34] M. Dvoyashkin, A. Wang, S. Vasenkov, and C. R. Bowers, Xenon in l-alanyl-l-valine nanochannels: A highly ideal molecular single-file system, J. Phys. Chem. Lett. **4**, 3263 (2013).

[35] A. Ryabov, *Stochastic Dynamics and Energetics of Biomolecular Systems*, Springer Theses (Springer, Cham, 2016).

[36] P. Dolai, A. Das, A. Kundu, C. Dasgupta, A. Dhar, and K. V. Kumar, Universal scaling in active single-file dynamics, Soft Matter **16**, 7077 (2020).

[37] R. Wittmann, H. Löwen, and J. M. Brader, Order-preserving dynamics in one dimension – single-file diffusion and caging from the perspective of dynamical density functional theory, Mol. Phys. **119**, e1867250 (2021).

[38] T. Banerjee, R. L. Jack, and M. E. Cates, Role of initial conditions in one-dimensional diffusive systems: Compressibility, hyperuniformity, and long-term memory, Phys. Rev. E **106**, L062101 (2022).

[39] H. van Beijeren, K. W. Kehr, and R. Kutner, Diffusion in concentrated lattice gases. III. Tracer diffusion on a one-dimensional lattice, Phys. Rev. B **28**, 5711 (1983).

[40] N. Leibovich and E. Barkai, Everlasting effect of initial conditions on single-file diffusion, Phys. Rev. E **88**, 032107 (2013).

[41] R. J. Baxter, Percus–Yevick equation for hard spheres with surface adhesion, J. Chem. Phys. **49**, 2770 (1968).

[42] J. K. Percus, One-dimensional classical fluid with nearest-neighbor interaction in arbitrary external field, J. Stat. Phys. **28**, 67 (1982).

[43] J.-B. Delfau, C. Coste, and M. Saint Jean, Single-file diffusion of particles with long-range interactions: Damping and finite-size effects, Phys. Rev. E **84**, 011101 (2011).

[44] P. M. Centres and S. Bustingorry, Effective edwards-wilkinson equation for single-file diffusion, Phys. Rev. E **81**, 061101 (2010).

[45] A. M. Fouad and J. A. Noel, On the role of adhesion in single-file dynamics, Physica A **480**, 1 (2017).

[46] A. P. Antonov, S. Schweers, A. Ryabov, and P. Maass, Brownian dynamics simulations of hard rods in external fields and with contact interactions, Phys. Rev. E **106**, 054606 (2022).

[47] M. A. Miller and D. Frenkel, Simulating colloids with Baxter's adhesive hard sphere model, J. Phys.: Condens. Matter **16**, S4901 (2004).

[48] M. A. Miller and D. Frenkel, Phase diagram of the adhesive hard sphere fluid, J. Chem. Phys. **121**, 535 (2004).

[49] The simulations have been performed under periodic boundary conditions for typical system sizes of 800σ. To obtain good numerical accuracy, averages were taken over 250 equilibrated initial particle configurations. At stickiness $\gamma = 10$, the CPU time for a simulation run of one configuration was 5 h for $\rho\sigma = 0.25$ and 45 h for $\rho\sigma = 0.8$ on one core of an AMD EPYC 7742 processor.

[50] Z. W. Salsburg, R. W. Zwanzig, and J. G. Kirkwood, Molecular distribution functions in a one–dimensional fluid, J. Chem. Phys. **21**, 1098 (1953).

[51] Y. Tago and S. Katsura, The Percus–Yevick equation of state for the sticky hard rod gas, Can. J. Phys. **53**, 2587 (1975).

[52] S. B. Yuste and A. Santos, Radial distribution function for sticky hard-core fluids, J. Stat. Phys. **72**, 703 (1993).

[53] See Supplemental Material at http://link.aps.org/supplemental/10.1103/PhysRevE.107.L042102, which includes Ref. [56], for the derivation of the geometric cluster size distribution in Eq. (7), the verification of the scaling (11) of the mean squared displacement for fixed cluster sizes after equilibration, and the derivation of the coefficient $D_{1/2}$ in Eq. (12).

[54] K. Misiunas and U. F. Keyser, Density-Dependent Speed-up of Particle Transport in Channels, Phys. Rev. Lett. **122**, 214501 (2019).

[55] M. Driscoll and B. Delmotte, Leveraging collective effects in externally driven colloidal suspensions: Experiments and simulations, Curr. Opin. Colloid Interface Sci. **40**, 42 (2019).

[56] G. Nägele, On the dynamics and structure of charge-stabilized suspensions, Phys. Rep. **272**, 215 (1996).